

On Sinai billiards on flat surfaces with non-flat horns

Henk Bruin *

July 21, 2022

Abstract

We show that certain billiard flows on planar billiard tables with horns can be modeled as suspension flows over Young towers with exponential tails. Because the height function of the suspension flow itself is polynomial when the horns are Torricelli-like trumpets, one can derive Limit Laws for the billiard flow, including Stable Limits if the parameter of the Torricelli trumpet is chosen in $(1, 2)$.

Mathematics Subject Classification (2010): Primary: 37D50, Secondary: 37A25, 37A60

Keywords. billiards, suspension flow, limit laws, decay of correlations

1 Introduction

Recent results on the statistical properties of non-uniformly hyperbolic flows in dynamical systems include polynomial mixing rate, when the flow can be modeled as suspension flow over a Gibbs-Markov map or over a Young tower, and the roof function h of the suspension flow has polynomial tails:

$$\mu(\{x \in M : h(x) > t\}) = \ell(t)t^{-\beta}, \quad (1)$$

where $\ell(t)$ is a slowly varying function. There are geodesics flows on non-compact surfaces of curvature -1 where the above tail condition with $\beta = 1$ or 2 applies (although properties of Kleinian groups rather than Young towers are used in the modeling). For Lorentz gas with infinite horizon, we get tail behavior with $\beta = 1$ or $\beta = 2$, depending on the dimension of the lattice of the scatterers. So, although the theory puts no restriction on the parameter β in (1), classical examples provide us only with very specific values of β . In dimension 1, the Pomeau-Manneville maps allow for inducing schemes where the induce time satisfies (1) for $\beta = 1/\alpha$ and α is the order of contact between the graph and the tangent at the neutral fixed point. Thus $\beta > 0$ can be chosen freely, but despite some higher-dimensional variants, Pomeau-Manneville maps remain too specific to play a substantial role in the modeling of billiards or other mechanical models. In [17, 18, 6] it was shown that almost Anosov diffeomorphisms (and flows [7]) also allow inducing schemes with tails satisfying (1). These are non-uniformly hyperbolic invertible systems,

*Faculty of Mathematics, University of Vienna, Oskar Morgensternplatz 1, 1090 Vienna, Austria;
henk.bruin@univie.ac.at

and, in contrast to Pomeau-Manneville maps, can be chosen to be C^∞ or real analytic, even if β is non-integer.

The purpose of this paper is to provide a class of examples that fit directly in the context of billiard maps, and which can be modeled by suspension flows over Young towers with tails as in (1). The basic ingredient is the geodesic flow over a surface of revolution, which we call *horns*, of which the pseudo-sphere and the Torricelli trumpet are examples. The pseudo-sphere has constant curvature -1 ; in fact it is the largest manifold with this property that can be embedded in \mathbb{R}^3 , [16]. Pseudo-spheres are part of non-compact hyperbolic surfaces with cusps, such as the “three-horned sphere”. As such, they are covered by the classical theory of geodesic flows on surfaces of curvature -1 , and they lead to exponential tails. “New” (or at least we are not aware of explicit calculations in the literature) is a one-parameter family of Torricelli trumpets, which provide tails as in (1) where the exponent β is equal to the parameter of the family.

Let the billiard table \mathcal{Q} be a flat compact manifold, such as a torus or a rectangle with reflecting boundaries. We assume that there are multiple convex scatterers O_i with C^3 boundaries and curvature bounded away from zero. Disks will do. These are “hard balls”, i.e., the collision rule of the particle with such scatterers is the rule of fully elastic reflection. Also, the scatterers have disjoint closures and there are enough of them that the horizon is finite. Additionally we replace finitely many disk-shape neighborhoods in $\mathcal{Q} \setminus \cup_i O_i$ horns H_j , but always such that there is no straight line between horns without a scatterer in between. Thus ∂H_j are circles in \mathcal{Q} , say with radius r_0 , and a particle that exits a horn first meets a regular scatterer before entering another horn. Thus the “horizon”, i.e., the maximal flight time τ_{\max} between collisions is finite, and since the O_i 's and H_j 's have disjoint closures, also the minimal flight time between collisions $\tau_{\min} > 0$.

A unit mass, unit speed particle moves on this surface with scatterers. It reflects fully elastically at the scatterers, but when it meets a horn H_j , it moves up inside the horn (cf. Figures 1 and 5), keeping its speed but observing the law of preservation of angular momentum and the holonomic constraint keeping it in H_j , until it exits H_j again and resumes its trajectory on \mathcal{Q} . The excursion time is $2t_{\max}(\varphi_0)$ where $\varphi_0 \in [\frac{\pi}{2}, \frac{\pi}{2}]$ is the angle of incidence that the particle's trajectory makes with the normal vector to ∂H , and t_{\max} is the time for an excursion to reach the highest point in the horn. Due to the radial symmetry of H_j , the angle of reflection $\varphi_1 = -\varphi_0$. We denote the flow on $\mathcal{Q} \cup \bigcup_j H_j$ by ϕ^t .

One can consider the horn as a “soft-ball” scatterer in the sense that it does reflect the particle, but not according to the law of elastic collision: although the angle of incidence equals the angle of reflection (up to a minus sign: $\varphi_1 = -\varphi_0$), the point of entrance on ∂H is not the point of exit. (However, the excursions of the particle in the horn can take an unbounded amount of time, and the effects of this resemble the effects of infinite horizon Lorentz gas.) Let us parametrize the circle ∂H_j by the angle θ . The exit angle θ_1 is a function of the entrance angle θ_0 and the angle of incidence φ_0 . The angle displacement¹

$$\theta_1 - \theta_0 =: \Delta\theta = \Delta\theta(\varphi_0)$$

depends on φ_0 but (due to radial symmetry) not on θ_0 . Since $\varphi_1 = -\varphi_0$, the resulting reflection map

$$R : M \rightarrow M, \quad (\theta_0, \varphi_0) \mapsto (\theta_0 + \Delta\theta(\varphi_0), -\varphi_0) \quad M := \left(\bigcup_i \partial O_i \cup \bigcup_j \partial H_j \right) \times \left[-\frac{\pi}{2}, \frac{\pi}{2} \right],$$

¹called rotation function in [4]

represents the outgoing position and angle as function of the incoming position and angle. Note that $\Delta\theta(\varphi_0) = 0$ at scatterers. Let the flight map $F : M \rightarrow M, (\theta_1, \varphi_1) \mapsto (\theta_0, \theta_0 + \varphi_1 - \theta_1)$ take the outgoing coordinates (θ_1, φ_1) from one horn (or scatterer) to the incoming coordinates (θ_0, φ_0) of the next. The composition $T = R \circ F$ is the billiard map, expressed in outgoing coordinates from one horn or scatterer to the next.

For lack of a better word, we call these systems billiard flows on a flat table with horns. The horns we choose are Torricelli-like trumpets, pseudo-spheres and spherical sections, covered in Sections 3.3, 3.4 and 3.5, respectively. As usual in billiards, $T = R \circ F$ preserves a measure μ that is absolutely continuous to Lebesgue measure, with density $d\mu = \cos \varphi_1 d\theta_1 d\varphi_1$. With respect to this measure, Sinai billiards (both map and flow) are known to be ergodic, mixing and even Bernoulli, [8, 15, 22]. Our setting is similar enough to conclude mixing (see [10, Section 6.7]), but that doesn't give any quantitative result.

Theorem 1.1 *The billiard flow on billiard tables with horns can be modeled as a suspension flow over a Young tower with exponential tails, see Section 2.4. The height function h of the suspension*

1. *has polynomial tails $\mu(\{x \in M : h(x) > t\}) \sim Ct^{-\beta}$ for some constant $C > 0$ if the horns² are Torricelli trumpets with $\beta > 0$ equal to the parameter of the trumpet.*
2. *has exponential tails if the horns are pseudo-spheres.*
3. *is bounded above if the horns are sections of spheres.*

It follows that the billiard map has non-zero Lyapunov exponents. The value of this theorem lies in giving exponential mixing rates for the billiard map, and limit laws of the flow w.r.t. the Liouville measure. We state these results later on (Theorem 2.1 and 3.1) as they can be taken from the literature. The literature so far only partially covers mixing rates for flows, so we will make no undue speculations in that direction. Although soft-ball billiards will be one of our main tools, the flow on Torricelli trumpets and pseudo-spheres are in fact flows on negatively curved surfaces (in case of the Torricelli trumpet, the curvature tends to zero in the cusp). There is extensive literature on such flows, e.g. [11, 12, 14, 20] and references therein to give a sample, but these are predominantly concerned with ergodicity, mixing and Lyapunov exponents. The application to limit laws, and the exact computations of our types of horns (despite similarities to [20, Section 2]) seem to be new.

The next section is concerned with building a Young tower for the billiard map, or rather verifying that the methods of Chernov [9] and the soft-ball billiard approach of Bálint & Tóth [4, 5] applies under appropriate conditions. In Section 3.1 we then estimate the sojourn times on horn, that lead to the height of the suspension flow of Theorem 1.1.

Notation: We will write (θ, φ) for the angle and position at incoming collisions, and use (θ_0, φ_0) only if we want to emphasize that it is about the incoming collision (and then $(\theta_1, \varphi_1) = R(\theta_0, \varphi_0) = (\theta_0 + \Delta\theta(\varphi_0), -\varphi_0)$ is used for the outgoing collision). We write $a_n \sim b_n$ if $\lim_n a_n/b_n = 1$ and $a_n \approx b_n$ if a_n/b_n have a bounded and positive lim sup and lim inf.

Acknowledgments: HB gratefully acknowledges the support of FWF grant P31950-N45. He also wants to thank Péter Bálint for his explanations of his and Chernov's papers [4, 5, 9], and Homero Canales for verifying some of the lengthier computations in this paper.

²The statistical behavior is governed by the trumpet with the smallest parameter.

2 Billiard maps for tables with horns

2.1 Conditions to build a Young tower

The proof of exponential decay of correlation of Sinai billiard and various other billiards was achieved by Chernov [9] by building a Young tower with exponential tails, see [24]. For this, he states some technical conditions that ensure the existence of such a tower. One is the uniform hyperbolicity of the billiard map, so (despite its discontinuities) with uniform expansion and contraction rates, and the angles between stable and unstable leaves uniformly bounded away from zero. We discuss this for our setting in Proposition 2.1 and Section 2.3. Also distortion is to be bounded within homogeneity strips. Global distortion control is impossible due to grazing collisions (i.e., collisions with $\varphi = \pm\frac{\pi}{2}$) at scatterers. Homogeneity strips are therefore introduced in the phase space near $\varphi = \pm\frac{\pi}{2}$ within which distortion control is feasible. This leads, however, to the chopping of unstable leaves and the need for a “growth of unstable manifold” condition in [9, Section 2]. We discuss this for our setting in Section 2.4.

In their turn, Bálint & Tóth give Definitions 2 and 3 of [4] sufficient conditions in the soft-ball scatterer setting to apply the methods of Chernov. We summarize these conditions, using their notation, specifically the derivative of the angle displacement $\Delta\theta$:

$$\kappa(\varphi) = \frac{d}{d\varphi} \Delta\theta(\varphi).$$

1. $\inf_{\varphi} |2 + \kappa(\varphi)| > 0$.
2. $\tau_{\min} > \sup_{\varphi} -2r_0 \frac{\kappa(\varphi)}{\omega(\varphi)}$ where r_0 is the radius of the scatterers and $\omega(\varphi) = \frac{2+\kappa(\varphi)}{\cos \varphi}$.
3. $\Delta\theta$ is piecewise Hölder, i.e., there is $C > 0$ and $\alpha \in (0, 1)$ such that

$$|\Delta\theta(\varphi) - \Delta\theta(\varphi')| \leq C|\varphi - \varphi'|^{\alpha}$$

for all φ, φ' is the same element of a finite partition of the phase space.

4. $\Delta\theta$ is piecewise C^2 on the interiors of the partition in the previous item.
5. There is $C > 0$ such that $|\frac{d\kappa(\varphi)}{d\varphi}| \leq C|2 + \kappa(\varphi)|^3$.
6. There is $\varepsilon > 0$ such that $\omega(\varphi)$ from item 2. is monotone on one-sided neighborhoods $[\varphi^* - \varepsilon, \varphi^*)$ and $(\varphi^*, \varphi^* + \varepsilon]$ of angles φ^* where κ is infinite or discontinuous.

We list some comments on these properties, and mention where in this paper they are addressed further.

- ad 1. This condition fails for all the horns we consider, and this compromises the hyperbolicity of the billiard map, or more directly the dispersive nature of the collisions with horns. Our solution here is to insert extra scatterers, positioned at sufficient distance from the horn to make up for their lack of dispersion, see Section 2.2.
- ad 2. Since $\kappa(\varphi) = -2$ for some $\varphi \in [-\frac{\pi}{2}, \frac{\pi}{2}]$ for all the horns we consider, also this condition fails. However, it is used only to get sufficient dispersion of wavefronts, and our solution in Section 2.2 replaces the need for item 2.
- ad 3. Hölder continuity of the angle displacement $\Delta\theta(\varphi)$ holds in our case for $\varphi \approx \pm\frac{\pi}{2}$, but fails for $\varphi \approx 0$, i.e., the head-on collision with the horn. In fact, if $\varphi = 0$, the particle will never leave the horn again. As we will see, $\Delta\theta(\varphi)$ blows up near the discontinuity $\varphi = 0$, and this requires the largest adjustment to the argument in [4].

A second issue is the unboundedness of $\Delta\theta$ (and hence of κ) near head-on collisions with horns (i.e., angle of incidence $\varphi \approx 0$). This situation is not covered in [5]; it requires extra arguments (in the shape of adding more “homogeneity strips”) to control the distortion. However, we expect the largest expansion in this neighborhood to help in overcoming the effects of the extra chopping that this entails. Indeed, for fixed angle of entry θ_0 , we can partition a punctured neighborhood of $\varphi_0 = 0$ into intervals I_j such that the exit angle θ_1 ranges from 0 to 2π on each I_j . Unstable leaves become automatically long in this way, and there is no need for growth lemmas. However, we need to compute distortion of $\Delta\theta(\varphi)$ on these I_j , see Proposition 2.3.

- ad 4. The angle displacement $\Delta\theta(\varphi)$ is C^2 on all the intervals of continuity in $[-\frac{\pi}{2}, \frac{\pi}{2}]$. Because $\Delta\theta(\varphi)$ blows up near $\{\varphi = 0\}$, we have to resort to C^2 smoothness on the (artificial) homogeneity strips near $\{\varphi = 0\}$, but this is unproblematic.
- ad 5. This is unproblematic; the computations of our three types of horns yield this condition automatically, see Sections 3.3-3.5.
- ad 6. Again unproblematic; the computations of our three types of horns yield this condition automatically, see Sections 3.3-3.5.

2.2 Wavefronts and hyperbolicity

The horns can be interpreted as “soft balls”, and this allows us to adapt the approach of Bálint & Tóth [4, 5], We start our analysis showing that the billiard map is hyperbolic. The hyperbolicity proof consists foremost of an analysis of wave fronts, specifically their focusing and defocusing nature, and how these are altered by a collision. It is the defocusing fronts that indicate the unstable directions of the billiard map T ; the stable directions are then given by the defocusing fronts of the inverse T^{-1} .

The property of a soft ball scatterer is that the entrance and exit positions of a particle are not the same; for round scatterers the difference is expressed as a difference in angles $\Delta\theta$, which is a function of the angle of incidence φ . The key quantity is the derivative $\kappa(\varphi) = \frac{d}{d\varphi}\Delta\theta(\varphi)$. If $\kappa(\varphi) \notin [-2, 0]$, defocused wavefronts remain defocused in the collision. If $\kappa(\varphi) \in [-2, 0]$ then the wave front can start to focus during the free flight. However, $\kappa(\varphi)$ is not too close to -2 and the distance between the scatterers sufficiently large, then wave fronts can focus, go “through the focus” and then defocus again before reaching the next scatterer, see Figure 1. In [4] the conditions for this mechanism is captured in Definition 2, which gives conditions on the distortion of $\kappa(\varphi)$, and its values in connection to the distance between scatterers.

In detail, we need Definition 2 in [4], which we restated as items 1. and 2. in Section 2.1. For the elastic scatterers O_i , the displacement in collision angle $\Delta\theta(\varphi) \equiv 0$, so $\kappa(\varphi) \equiv 0$, and the above conditions follow automatically as long as $\tau_{\min} > 0$.

In the Section 3.1, we compute sojourn times as well as $\Delta\theta(\varphi)$ and $\kappa(\varphi)$ for horns of various types. An important conclusion is that the range of κ includes the interval $[-2, 0]$ entirely, as φ varies from $-\frac{\pi}{2}$ to $\frac{\pi}{2}$, so the mechanism of collision-focusing-defocusing-collision cannot hold everywhere. But since there will be a hard scatterer between every two excursions in a horn, wave fronts that are so close to parallel fronts when they leave a horn that they cannot defocus before the next scatterer, will collide with a hard scatterer and then become defocused. In Proposition 2.1 we quantify this mechanism, and determine the minimal distances between scatterers to guarantee uniform hyperbolicity of the billiard map.

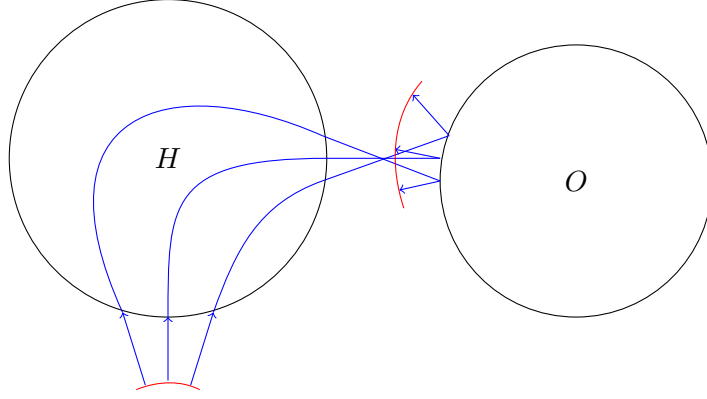


Figure 1: A focusing-defocusing wave front between collisions with a horn and a scatterer.

Proposition 2.1 *Assume that the distance between the horn H and any scatterer O is at least $2r_H r_O$ (where r_H and r_O are the radii of H and O respectively). Then the billiard map is hyperbolic.*

Proof. We follow the argument and notation of [4, Section 2] on the behavior of wavefronts at scatterers. Let q_- parametrize the wavefront W_- coming from the horn H and approaching the scatterer O , so q_- and $q_- + dq_-$ are to infinitesimally close points on W_- with unit velocity vectors v_- and $v_- + dv_-$. Note that W_- is parallel if $\frac{dv_-}{dq_-} = 0$ and focusing if $\frac{dv_-}{dq_-} < 0$. After collision, we obtain point q_+ and $q_+ + dq_+$ on the outgoing wavefront W_+ , with velocities v_+ and $v_+ + dv_+$, see Figure 2 left.

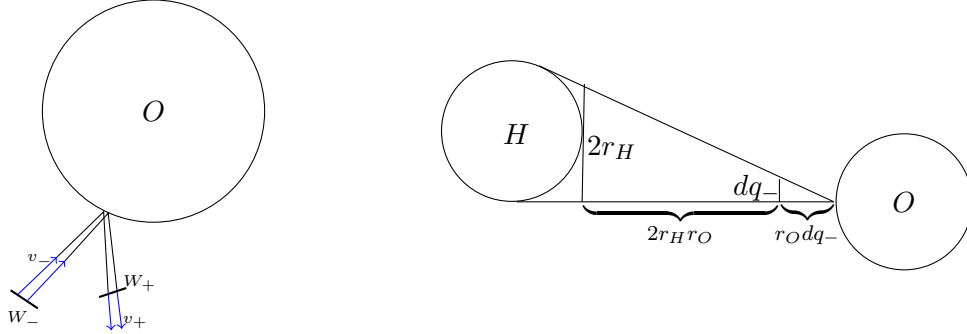


Figure 2: Wavefronts and congruent triangles

Since for a scatterer $\Delta\theta(\varphi) = 0$ and hence $\kappa(\varphi_0) = 0$, [4, Formula (3.2)] gives

$$dq_+ = dq_-, \quad dv_+ = dv_- + \frac{2}{r_H \cos \varphi} dq_-.$$

Note here that in the formula for dv_+ we get a plus-sign (as opposed to [4, Formula (3.2)]) because we parametrize W_+ in Figure 2 in the opposite way of [4, Figure 1]. If $\frac{dv_-}{dq_-} \geq -\frac{1}{r_H}$, then $\frac{dv_+}{dq_+} > \frac{1}{r_O}$, so the outgoing front is dispersive. If $\frac{dv_-}{dq_-} < -\frac{1}{r_O}$, then extrapolating backwards and using that the distance between H and O is $> 2r_H r_O$, congruence of triangles (see Figure 2 (right)) shows that the wavefront leaving H is actually wider than H itself. This means that the actual wavefront W_- focuses before it reaches the scatterer O . \square

2.3 Distortion control of the reflection map R near $\{\varphi = 0\}$.

In this section, we study the distortion of the billiard map T . Since the flight component F has bounded distortion, and the reflection at scatterers goes as in the standard billiard maps (with homogeneity strips as in [9]), we concentrate on the reflection map R . Here the distortion near $\varphi \approx 0$ is not an issue; the problem occurs for $\varphi \approx 0$ because $\Delta\theta$ and hence κ are unbounded here. Our solution is as with grazing collisions at scatterers, introduce so-called homogeneity strips within which distortion is controlled. Fortunately, the large expansion in such strips overcomes the artificial chopping by such strips immediately, and hence the analysis of this case is easier, and doesn't require growth lemmas. We start this section by describing the homogeneity regions, and then deal with the distortion control, with Proposition 2.3 as main result.

For each horn H_j select a scatterer O_j opposite to it. The line connecting the centers of H_j and O_j contains a trajectory $\phi^t(x)$ such that $x \in \partial O_j$ and $\lim_{t \rightarrow \pm\infty} \phi^t(x) = C_j$, the center of H_j . This trajectory meets no other scatterers or horns. There is a maximal arc A_j in ∂H_j such that the billiard map $T^2(A_j \times \{0\}) \subset \partial H_j \times [-\frac{\pi}{2}, \frac{\pi}{2}]$, i.e., a particle starting in $A_j \subset \partial H_j$ with outgoing angle $\varphi = 0$ hits ∂H_j again at the second iterate of the billiard map, bouncing once against O_j in between, see Figure 3.

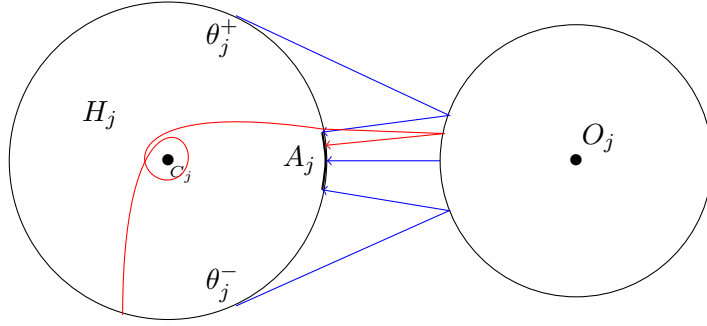


Figure 3: Trajectories asymptotic to the center C_j of H_j .

Let $A'_j = F \circ T(A_j \times \{0\})$; it is a smooth curve in $M_j := \partial H_j \times [-\frac{\pi}{2}, \frac{\pi}{2}]$ that stretches across M_j in the vertical direction and is transversal to $\{\varphi = 0\}$. Let $a_j^- = (\theta_j^-, +\frac{\pi}{2})$ and $a_j^+ = (\theta_j^+, -\frac{\pi}{2})$ be the endpoints of A'_j . The reflection map

$$R : M_j \setminus \{\varphi = 0\} \rightarrow M_j \setminus \{\varphi = 0\}, \quad (\theta, \varphi) \mapsto (\theta + \Delta\theta(\varphi), -\varphi),$$

is a bijection. The closer to the equator $\partial H_j \times \{0\}$, the stronger the shear of R . That is, an arc $\{\theta\} \times (0, \frac{\pi}{2}]$ is mapped by F to a spiral curve wrapping infinitely often around the annulus M_j , compactifying on $\partial H_j \times \{0\}$ from below, while $\{\theta\} \times [-\frac{\pi}{2}, 0)$ is mapped by R to a spiral curve wrapping infinitely often around the annulus M_j , compactifying on $\partial H_j \times \{0\}$ from above. Conversely, $\Psi_j := R^{-1}(A'_j \setminus \{\varphi = 0\})$ consists of two spirals wrapping infinitely often around M_j and compactifying on the equator, one from above and one from below. For every point $(\theta, \varphi) \in \Psi_j$, $F \circ R(\theta, \varphi)$ represents a particle outgoing from O_j and head-on colliding with H_j , so that $T \circ F \circ R(\theta, \varphi)$ is not defined: the particle never leaves H_j again.

Now $M_j \setminus \overline{\Psi_j}$ consists of two strips that wrap around M_j infinitely often and approaching $\{\varphi = 0\}$ in a spiral fashion from above and below. Let $\psi_j^+ = R^{-1}(a_j^+)$, and let E_j be the straight line connecting ψ_j^- and ψ_j^+ in M_j . Then E_j cuts $M_j \setminus \overline{\Psi_j}$ into infinitely many

strips $I_{\pm k}$, $k \in \mathbb{N}$, whose closures are curvilinear rectangles except that they coincide at two opposite corners; note that they wrap around M_j once.

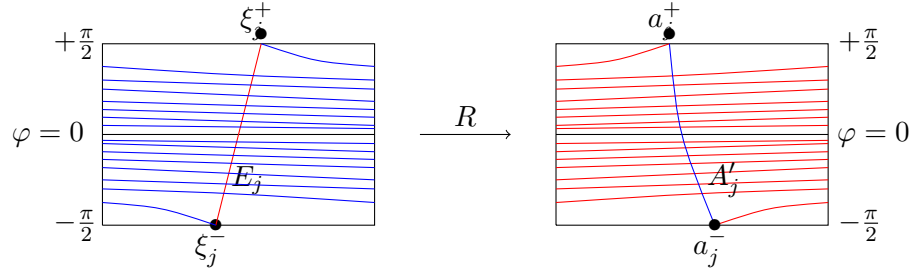


Figure 4: The curves Ψ_j , E_j and $R(\Psi_j)$, $A'_j = R(\Psi_j)$ in M_j .

The set $I_{\pm k}$ play the role of homogeneity strips, within which unstable derivatives are uniformly bounded.

Lemma 2.1 *Let $\tilde{I}_{\pm k}$ be the projections of $I_{\pm k}$ into $\{0\} \times [-\frac{\pi}{2}, \frac{\pi}{2}]$. Then $|\tilde{I}_{\pm k}| \approx k^{-(1+\frac{1}{\beta})} = o(d(\tilde{I}_k, 0))$ as $k \rightarrow \infty$ for some $\beta > 0$, where d is the Euclidean distance on $[-\frac{\pi}{2}, \frac{\pi}{2}]$.*

Proof. The precise computation depends on the shape of the horn H_j , but there is always a leading term of the map $\Delta\theta : [-\frac{\pi}{2}, \frac{\pi}{2}] \rightarrow \mathbb{R}$ of the form $g : \varphi \mapsto C\varphi^{-\beta}$ for some $0 \neq C \in \mathbb{R}$ and $\beta > 0$. Now

$$\tilde{I}_k \sim g^{-1}(2\pi k, 2\pi(k+1)) = \left(\left(\frac{C}{2\pi k}\right)^{1/\beta}, \left(\frac{C}{2\pi(k+1)}\right)^{1/\beta} \right),$$

so $|\tilde{I}_k| \sim \left(\frac{C}{2\pi k}\right)^{1/\beta} \frac{1}{\beta k} \sim \frac{1}{\beta k} d(\tilde{I}_k, 0)$. The same argument works for $-k$. \square

Proposition 2.2 *(Un)stable leaves are uniformly transversal to the coordinate axes: there is $C_{tran} > 0$ such that*

$$\frac{1}{C_{tran}} \leq \frac{dw^{u/s}(\varphi)}{d\varphi} \leq C_{tran},$$

for all (un)stable leaves $w^{u/s}(\varphi)$ parametrized as function of the outgoing angle. Also the angles between stable and unstable curves are uniformly bounded away from zero.

Proof. Let us use coordinates $(d\theta, d\varphi)$ for the tangent space $T_{(\theta, \varphi)}$ (at outgoing angles). In the theory of elastic (hard) convex scatterers, the (un)stable cone-fields

$$\mathcal{C}_{(\theta, \varphi)}^u := \{d\theta \cdot d\varphi \geq 0\} \quad \text{and} \quad \mathcal{C}_{(\theta, \varphi)}^s := \{d\theta \cdot d\varphi \leq 0\} \quad \text{are invariant} \quad (2)$$

under DT and DT^{-1} respectively, see [9, Section 6]. Basically, the reflection changes the sign of the angle, and fixes the position, so that $d\varphi^+ = -d\varphi^-$ and $d\theta^+ = d\theta^-$. Then the next collision incoming at $(\theta_1^-, \varphi_1^-)$ reverses orientation again, because $d\varphi_1^- = \psi - d\varphi^+$ (where ψ is the angle between the normal vectors at θ and θ_1), and $d\theta_1^- = (1 + \kappa(\theta^+))(1 + \kappa(\theta_1^-))\tau(\theta^+, \varphi)d\theta_1^-$. Here κ denotes the curvature at the boundary of the scatterers, and $\tau(\theta^+, \varphi^+)$ is the flight time associated with the billiard map T .

For horns we have $d\varphi^+ = -d\varphi^-$ and $d\theta^+ = d\theta^-$ because $\theta^+ = \theta^- + \Delta\theta$. Also DT maps $\mathcal{C}_{(\theta,\varphi)}^u$ strictly into $\mathcal{C}_{T(\theta,\varphi)}^u$ and DT^{-1} maps $\mathcal{C}_{(\theta,\varphi)}^s$ strictly into $\mathcal{C}_{T^{-1}(\theta,\varphi)}^s$. Therefore (un)stable leaves $W^{u/s}$ are transversal to the level sets $\{\theta = \text{Const.}\}$ and $\{\varphi = \text{Const.}\}$.

The discussion so far dealt with the strict invariance of the unstable cone-field $\{d\theta \cdot d\varphi \geq 0\}$. It remains to establish the strictly positive constant C_{tran} . But here (6.1)-(6.4) in [9] for both scatterers and horns apply with no other change than that the variable r is called θ in our setting.

The same argument applies to stable leaves as well, and since stable and unstable curves belong to disjoint cones, uniform transversality between stable and unstable leaves follows. \square

The backward singularity sets $S^{-m} := T^{-m}(\bigcup_i \partial O_i \times \{-\frac{\pi}{2}, \frac{\pi}{2}\} \cup \bigcup_j \partial H_j \times \{0\})$ for $m \geq 1$, also belong to the stable cone field, and the forward singularity sets $S^m := T^m(\bigcup_i \partial O_i \times \{-\frac{\pi}{2}, \frac{\pi}{2}\} \cup \bigcup_j \partial H_j \times \{0\})$ for $m \geq 1$, belong to the unstable cone field, see [9, Section 6].

Proposition 2.3 *Let W be an unstable leaf contained in $I_{\pm k}$ and bounded away from $\{\varphi = \pm \frac{\pi}{2}\}$. Then there is $C_{\text{dist}} \in \mathbb{R}$ such that the distortion in the unstable direction*

$$\log \frac{|J^u R(y)|}{|J^u R(x)|} \leq C_{\text{dist}} d_{R(W)}(R(x), R(y)), \quad (3)$$

where $d_{R(W)}$ indicates arc-length in $R(W)$. In fact, $\log \frac{|J^u R(y)|}{|J^u R(x)|} = o(d_{R(W)}(R(x), R(y)))$ as $k \rightarrow \infty$, i.e., as $\varphi \rightarrow 0$.

Proof. First we assume that W is transversal to horizontal lines in M , i.e., transversal to lines of constant φ . Thus W can be written as the graph of a C^1 -function $w : \tilde{I}_{\pm k} \rightarrow \partial H_j$. The length-element of arc-length along W is $ds = ds(\varphi) = \sqrt{1 + (w'(\varphi))^2}$. Recall that $R(\theta, \varphi) = (\theta + \Delta\theta(\varphi), -\varphi)$ is the reflection map, and $\Delta\theta'(\varphi) = \kappa(\varphi)$. Then the image of ds under R is

$$dR(s) = \sqrt{d\varphi^2 + (w'(\varphi) + \kappa(\varphi))^2} d\varphi^2 = \sqrt{1 + (w'(\varphi) + \kappa(\varphi))^2} d\varphi.$$

Transversality of W means that $|w'|$ is bounded, so

$$\frac{dR(s)}{ds} = \sqrt{1 + (w'(\varphi) + \kappa(\varphi))^2} \approx \kappa(\varphi) \approx C\beta\varphi^{-(\beta+1)}.$$

where we used that leading term of κ is $C\beta\varphi^{-(\beta+1)}$ as in Lemma 2.1. Hence, taking $x = (w(\varphi), \varphi)$ and $y = (w(\varphi + \varepsilon), \varphi + \varepsilon)$, the distortion

$$\log \frac{|J^u R(y)|}{|J^u R(x)|} \approx -(\beta + 1) \log\left(1 + \frac{\varepsilon}{\varphi}\right) \approx \frac{-\varepsilon(1 + \beta)}{\varphi}.$$

Now to find $d_{R(W)}(R(y), R(x))$ we integrate $dR(s)$ over $[\varphi, \varphi + \varepsilon]$. This gives

$$\begin{aligned} \int_{\varphi}^{\varphi+\varepsilon} \sqrt{1 + (w'(v) + \kappa(v))^2} dv &\approx \int_{\varphi}^{\varphi+\varepsilon} \kappa(v) dv \\ &= \Delta\theta(\varphi + \varepsilon) - \Delta\theta(\varphi) \approx C \left((\varphi + \varepsilon)^{-\beta} - \varphi^{-\beta} \right) \\ &= C\varphi^{-\beta} \left(\left(1 + \frac{\varepsilon}{\varphi}\right)^{-\beta} - 1 \right) \sim -\beta C\varepsilon\varphi^{-(1+\beta)}, \end{aligned}$$

where in the last approximation we used that $|\varepsilon|$ is small compared to $|\varphi|$ as shown in Lemma 2.1. Formula (3) follows.

For $\varphi \rightarrow 0$, we get $1 + \sup |w'|^2 = o(\kappa(\varphi))$, so that the \approx becomes \sim in this case, and the extra factor $\varphi^{-\beta}$ accounts for the little o . \square

Corollary 2.1 *The derivative on unstable manifolds in $I_{\pm k}$ satisfies:*

$$\frac{1}{C_{exp}} k^{1+\beta} \leq |J_W^u(x)| \leq C_{exp} k^{1+\beta}, \quad (4)$$

for some expansion constant $C_{exp} > 0$.

2.4 Building a Young tower with exponential tails

A Young tower [23] is a schematic dynamical system, in fact an extension over a dynamical system (X, T) , of the form $(\Delta, T_\Delta, \mu_\Delta)$, where the space

$$\Delta = \bigsqcup_i \Delta_i = \bigsqcup_i \bigsqcup_{\ell=0}^{\sigma_i-1} \Delta_{i,\ell},$$

where Δ_0 is a subset of X , partitioned into subsets $\Delta_{i,0}$ such that $T^{\sigma_i} : \cup_i \Delta_{i,0} \rightarrow \Delta_0$ is a Gibbs-Markov map (so uniformly hyperbolic), preserving an SRB-measure μ_0 . Here $r : \Delta_0 \rightarrow \mathbb{N}$ with $r|_{\Delta_{i,0}} =: \sigma_i$ constant for all i is called the roof function. The sets $\Delta_{i,\ell}$ are copies of the $\Delta_{i,0}$ and the tower map T_Δ acts as

$$T_\Delta : x \in \Delta_{i,\ell} \mapsto \begin{cases} x \in \Delta_{i,\ell+1} & \text{if } 0 \leq \ell < \sigma(x) - 1; \\ T^{\sigma(x)}(x) \in \Delta_0 & \text{if } \ell = \sigma(x) - 1, \end{cases}$$

and (Δ, T_Δ) factors over (X, T) via $\pi : \Delta \rightarrow X$, $\pi(x \in \Delta_{i,\ell}) = T^\ell(x)$. We speak of exponential tails if there is $\lambda \in (0, 1)$ such that $\mu_0(\{x : \sigma(x) > n\}) = O(\lambda^n)$. We can extend μ_0 to an T_Δ -invariant measure by setting $\mu_\Delta|_{\Delta_{i,\ell}} = \bar{\sigma}^{-1} \mu_0|_{\Delta_{i,0}}$ for normalizing constant $\bar{\sigma} = \sum_{n \geq 1} n \mu_0(\{\sigma(x) = n\})$. This measure pushes down to a T -invariant SRB-measure on (X, T) via $\mu = \mu_\Delta \circ \pi^{-1}$. The existence of a Young tower with exponential tails implies that the underlying system (X, T, μ) is exponentially mixing (provided $\gcd(\sigma_i : i \in \mathbb{N}) = 1$) and satisfies the Central Limit Theorem for Hölder observables, see [24].

Chernov [9, Theorem 2.1] proved a general theorem on the existence of a Young tower with exponential tails for non-uniformly hyperbolic invertible maps, based on a set of conditions concerning expansion and distortion control along unstable leaves and specific “growth of unstable manifolds” conditions (2.6)-(2.8) in [9]. He continues to verify these conditions for various billiard systems, of which the standard Sinai billiard maps³ is the most relevant to us, see [9, Section 6 & 7]. Bálint & Tóth verify the conditions for soft scatterers, leading them to condition Definition 3 in [5]. In the previous sections we verified most of the Chernov resp. Bálint & Tóth conditions, and here we combine these steps to the final verification. That is, we indicate which adaptations in the arguments of [9, Section 7] are still required.

Chernov [9, Section 7] uses two metrics to obtain hyperbolic expansion:

³i.e., disjoint strictly convex fully elastic scatterers with C^3 boundaries on a compact flat table, first fully treated in [23]

- The p -(pseudo-)metric which has the best expansion properties, but only that after a close-to-grazing collision with corresponding cut into homogeneity strips, the expansion has a one iterate delay. (Note that for horns, grazing collisions induce no discontinuities, so for the such homogeneity strips can be skipped.)
- The Euclidean metric. Now the expansion factor in unstable directions occurs instantaneously at collisions, but it is not always ≥ 1 . Therefore a particular iterate T^m of the billiard map T is chosen, which multiplies the number of discontinuity curves $\cup_{j=0}^{m-1} S^{-j}$ and $\cup_{n=0}^{m-1} T^{-n}(\cup_j \partial H_j \times \{0\})$, and corresponding boundaries of homogeneity strips $\cup_{k \geq k_0} \cup_{n=0}^{m-1} T^{-n}(\partial I_{\pm k})$.

However, combining the two metrics, one can prove uniform expansion (contraction) of unstable (stable) leaves, see [9, Lemma 7.1].

Let W be any unstable leave of length $\leq \delta_0$. It may be cut into at most $K_m + 1$ pieces by S^{-m} , where K_m depends only on m and the number of scatterers and horns. In the next m iterate, it may be cut again, even into countably many pieces, by curves in $\cup_{n=0}^{m-1} T^{-n}(\{\varphi = 0 \text{ at horns}\} \cup \{\varphi = \pm \frac{\pi}{2}\} \cup_{k \geq k_0} \partial I_{\pm k})$. We label these pieces as $W_{k_1, \dots, k_m, j}$, where $1 \leq j \leq K_m + 1$, $k_i \in \mathbb{Z}$ and $T^{m-n}(W_{k_1, \dots, k_m, j}) \subset I_{k_n}$. Bear in mind that some of these labels can refer to the empty set. Since horns and scatterers have their own homogeneity strips $I_{\pm k}$ where the expansion of the billiard map is $\approx k^{1+\beta}$ and $\approx k^2$ respectively, we will use $\nu := \min\{2, 1 + \beta\}$ for the worst case of the two. The unstable expansion for $T_1 = T^m$ on a piece W_{k_1, \dots, k_m} of unstable manifold thus becomes

$$|J_1^u(x)| \geq L_{k_1, \dots, k_m} := \max\{\Lambda_1, \frac{1}{C_{\text{exp}}} \prod_{k_i \neq 0} k_i^\nu\}.$$

This product $\prod_{k_i \neq 0}$ then reappears in the definition⁴ of $\Theta := 2 \sum_{k \geq k_0} k^{-\nu} \leq \frac{7}{\nu} \frac{1}{k_0^{\nu-1}}$. We need to choose k_0 so large that, as in [9, Formula (7.5)] with corresponding constant B_0 ,

$$(K_m + 1)(\Lambda_1^{-1} + 2B_0\Theta) < 1. \quad (5)$$

Also [9, Lemma 7.2] needs to be adjusted to:

Lemma 2.2 *For all $\delta > 0$, there is $B = B(m)$ such that*

$$\sum_{k_1, \dots, k_m \geq 2} \min\{\delta, (\kappa_1 \cdots \kappa_m)^{-\nu}\} < B(m) \delta^{\frac{\nu-1}{2m}}.$$

But the proof goes as in [9, Appendix], with some minor and obvious adaptations.

Thus we can apply Chernov's main theorem for the billiard map, which we restate here:

Theorem 2.1 *For any type of horn discussed in this paper, there are $\alpha, \lambda \in (0, 1)$ such that the billiard map (M, T) has exponential decay of correlations:*

$$\left| \int_M v \cdot w \circ T^n d\mu - \int_M v d\mu \int_M w d\mu \right| = O(\lambda^n)$$

for the SRB-measure μ and α -Hölder functions $v, w : M \rightarrow \mathbb{R}$ and also the Central Limit Theorem holds for v provided it is not cohomologous to a constant function.

⁴This Θ is called θ_0 in [9].

3 The billiard flow

The billiard flow can now be modeled as a suspension flow over this Young tower, i.e., the space is now $\Delta^h := \sqcup_{i,\ell} \Delta_{i,\ell} \times [0, h(x)] / \sim$ where $(x, h(x)) \sim (T_\Delta(x), 0)$, and the flow $\phi_\Delta^t(x, u) = (x, u + t) \in \Delta^h$. The height function h is either equal to the (bounded) flight time $\tau(x)$ between two scatterers, or equal to the flight time $\tau(x)$ between a scatterer and a horn plus the sojourn time $2t_{\max}(\varphi_0)$, where φ is the incoming angle at the collision with the horn. The ϕ_Δ^t -invariant measure $\mu_\Delta^h = \bar{h}^{-1} \mu_\Delta \otimes \text{Leb}$ for the normalizing constant $\bar{h} = \int_\Delta h(x) d\mu_\Delta$ or $\bar{h} = 1$ if this integral is infinite, because in this infinite measure case, there is no normalization. The corresponding flow-invariant measure μ^h is the push-down $\mu_\Delta^h \circ \pi_h^{-1}$ where $\pi_h(x, u) = \phi^u \circ \pi(x)$.

The computations in Section 3.3 show that the tails of h have the asymptotics

$$\mu(\{x \in M : h(x) > t\}) = \frac{1}{2\#(H_j \cup O_i)} \int_{\{x \in M : \tau(\theta, \varphi) + 2t_{\max}(\varphi) > t\}} \cos \varphi d\mu \sim Ct^{-\beta}$$

for some constant depending only on the shape of the horns and $\#(H_j \cup O_i)$ stand for the number of horns and scatterers. The actual flight time $\tau \in [\tau_{\min}, \tau_{\max}]$ doesn't feature in C . In fact, the exponent β is equal to the parameter β of the Torricelli trumpet, and therefore μ^h is finite if and only if $\beta > 1$.

We can apply results from [19] or [7] to derive the following distributional limit theorems for the flow.

Theorem 3.1 *Let $v \in L^1(\mu^h)$ be a Hölder observable. Then depending on the value of $\beta > 1$, we have the following limit theorems:*

- If $\beta > 2$, then v satisfies a standard Central Limit Theorem: provided v is not cohomologous to a constant function, there is a constant $\sigma > 0$ such that

$$\frac{1}{\sigma\sqrt{T}} \left(\int_0^T v \circ \phi^t dt - T \int v d\mu^h \right) \Rightarrow^d \mathcal{N}(0, 1) \quad \text{as } T \rightarrow \infty.$$

- If $\beta = 2$, then v satisfies a non-Gaussian Central Limit Theorem: provided v is not cohomologous to a constant function, there is a constant $\sigma > 0$ such that

$$\frac{1}{\sigma\sqrt{T \log T}} \left(\int_0^T v \circ \phi^t dt - T \int v d\mu^h \right) \Rightarrow^d \mathcal{N}(0, 1) \quad \text{as } T \rightarrow \infty.$$

- If $\beta \in (1, 2)$, then v satisfies a Stable Law:

$$\frac{1}{T^{1/\beta}} \left(\int_0^T v \circ \phi^t dt - T \int v d\mu^h \right) \Rightarrow^d G_\beta \quad \text{as } T \rightarrow \infty.$$

For the pseudo-sphere in Section 3.4, we get exponential tails for h , and for the sphere section in Section 3.5, h is bounded above. In these two cases, the billiard flow again satisfies the Central Limit Theorem, and is expected to have exponential decay of correlations (it is plausible that Dolgopyat's methods [13], see also [1, 2], apply).

3.1 Dynamics of the flow on horns

Let H be a surface of revolution in \mathbb{R}^3 obtained by revolving the curve $x = x(z)$ around the z -axis. We will use the radius $r = r(z) = \sqrt{x^2 + y^2}$ as radius of H and $z = z(r)$ is the inverse function. Thus H has the parametrization

$$\sigma(z, \theta) = (r(z) \cos \theta, r(z) \sin \theta, z), \quad z \geq z_0, \theta \in [0, 2\pi). \quad (6)$$

Abbreviate $r_0 := r(z_0)$.

Example 3.1 *The area and volume of H are*

$$A := 2\pi \int_{z_0}^{\infty} (1 + r'^2)r dz \quad \text{and} \quad V := \pi^2 \int_{z_0}^{\infty} r^2 dz$$

respectively. For $r(z) = z^{-\beta}$, we get $A = \infty$, $V = \frac{\pi}{2\beta-1} < \infty$ (*painter's paradox*) for $\beta \in (\frac{1}{2}, 1]$. This holds specifically for the case $\beta = 1$, i.e., $r = 1/z$, when H is called the *trumpet of Torricelli* (or *Gabriel's horn*, see Figure 5). For $\beta > 1$ we have $A, V < \infty$ and for $\beta \leq \frac{1}{2}$, both $A, V = \infty$. The Gaussian curvature of such a surface

$$\kappa_G = -\frac{r''}{r(1+r'^2)^2} = -\frac{\beta^2 + \beta}{z^2(1 + \beta^2 z^{-2(1+\beta)})^2} \text{ to } \quad \text{as } z \rightarrow \infty.$$

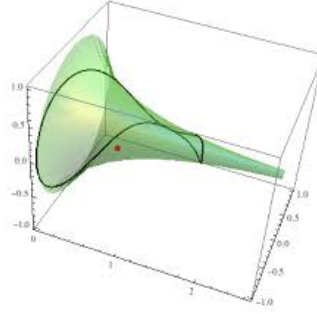


Figure 5: Geodesics on the pseudo-sphere.

For the next exposition, see [3, Section 4C]. A geodesic Γ is the path on H traced out by a unit mass particle moving along H at unit speed with no external forces other than the holonomic constraints keeping it on H . Assume the geodesic starts at $(z_0, \theta_0) \in \partial H$, making an incoming angle $\varphi_0 \in [-\frac{\pi}{2}, \frac{\pi}{2}]$ with the vertical meridian. The kinetic energy

$$E_{kin} = \frac{1}{2}|v|^2 = \frac{1}{2}((1 + r'^2)z^2 + r^2\dot{\theta}^2) = \frac{1}{2} \quad (7)$$

is one constant of motion. Due to the rotational symmetry (using Noether's Theorem), the z -component of the angular momentum

$$r^2\dot{\theta} = r_0|v| \sin \varphi_0 = r_0 \sin \varphi_0 \quad (8)$$

is the second constant of motion. Inserting $r\dot{\theta} = |v| \sin \alpha$ (where α is the angle with the vertical meridian) we get a derived constant of motion (Clairaut's Theorem)

$$r(z) \sin \alpha = r_0 \sin \varphi_0. \quad (9)$$

The value $\sin \alpha$ takes its largest value at the highest point of the geodesic (where $\sin \varphi_{\max} = 1$, $r_{\min} = r_0 \sin \varphi_0$, $\theta = \theta_{\max}$ and $z = z_{\max} = z(r_{\min})$), then the geodesic spirals down again (symmetrically to the upwards spiral), until it hits ∂H with an angle $\varphi_1 = -\varphi_0$.

The question we pose ourselves is:

What is the time t_{\max} needed of the geodesic particle to reach the top at z_{\max} ?

This has a direct consequence for the tails of geodesic flow if these sojourns inside the horns are modeled by suspension flow with height function $2t_{\max}$ and base map

$$R : M_j := \partial H_j \times [-\frac{\pi}{2}, \frac{\pi}{2}] \rightarrow M_j, \quad (\theta, \varphi) \mapsto (\theta + \Delta\theta(\varphi), -\varphi).$$

3.2 Computation of t_{\max} and θ_{\max}

From (7) combined with (8) we find

$$\dot{z} = \frac{dz}{dt} = \sqrt{\frac{1 - r(z)^2 \dot{\theta}^2}{1 + r'(z)^2}} = \sqrt{\frac{1 - r_0^2 r(z)^{-2} \sin^2 \varphi_0}{1 + r'(z)^2}}.$$

Therefore

$$dt = \sqrt{\frac{1 + r'(z)^2}{1 - r_0^2 r(z)^{-2} \sin^2 \varphi_0}} dz$$

and

$$t_{\max} = \int_0^{t_{\max}} dt = \int_{z_0}^{z_{\max}} \sqrt{\frac{1 + r'(z)^2}{1 - r_0^2 r(z)^{-2} \sin^2 \varphi_0}} dz.$$

Using the change of coordinates $u = \frac{r_0}{r(z)} |\sin \varphi_0|$, so $z = z(\frac{r_0 |\sin \varphi_0|}{u})$, $z = z_0 \Leftrightarrow u = |\sin \varphi_0|$, $z = z_{\max} \Leftrightarrow u = 1$ and $dz = -\frac{r_0 |\sin \varphi_0|}{u^2} \frac{1}{r'(z(\frac{r_0 |\sin \varphi_0|}{u}))} du$, we find⁵

$$t_{\max} = r_0 |\sin \varphi_0| \int_{|\sin \varphi_0|}^1 \frac{1}{u^2} \cdot \sqrt{\frac{1 + r'(z(\frac{r_0 |\sin \varphi_0|}{u}))^{-2}}{1 - u^2}} du. \quad (10)$$

Now for the displacement in angle θ between the initial angle θ_0 and the angle θ_{\max} reached at the top of the geodesic, we find, using (8) and the previous computation for \dot{z} :

$$\begin{aligned} \theta_{\max} - \theta_0 &= \int_{\theta_0}^{\theta_{\max}} d\theta = \int_0^{t_{\max}} \dot{\theta} dt = \int_0^{t_{\max}} \frac{r_0 \sin \varphi_0}{r^2} dt \\ &= \int_{z_0}^{z_{\max}} \frac{r_0 \sin \varphi_0}{r^2} \frac{1}{\dot{z}} dz \\ &= r_0 \sin \varphi_0 \int_{z_0}^{z_{\max}} \frac{1}{r^2} \sqrt{\frac{1 + r'(z)^2}{1 - r_0^2 r(z)^{-2} \sin^2 \varphi_0}} dz. \end{aligned}$$

This should be compared to Formula (5.2) in [4] expressing $\Delta\theta$ in terms of the potential of a soft scatterer. Applying the transformation $u = \frac{r_0}{r(z)} |\sin \varphi_0|$ as before, we get

$$\theta_{\max} - \theta_0 = \int_{|\sin \varphi_0|}^1 \sqrt{\frac{1 + r'(z(\frac{r_0 |\sin \varphi_0|}{u}))^{-2}}{1 - u^2}} du. \quad (11)$$

Throughout (and following the notation of [4, 5]) we let

$$\Delta\theta = 2(\theta_{\max} - \theta_0) = 2 \int_{|\sin \varphi_0|}^1 \sqrt{\frac{1 + r'(z(\frac{r_0 |\sin \varphi_0|}{u}))^{-2}}{1 - u^2}} du. \quad (12)$$

be the difference in incoming and outgoing angle of the obstacle as function of angle of incidence φ_0 . Its derivative w.r.t. φ_0 is denoted as

$$\begin{aligned} \kappa(\varphi_0) &= \frac{\partial \Delta\theta(\varphi_0)}{\partial \varphi_0} = -2 \operatorname{sgn}(\varphi_0) \sqrt{1 + (r'(z_0))^{-2}} - 2r_0 \operatorname{sgn}(\varphi_0) \cos \varphi_0 \times \\ &\int_{|\sin \varphi_0|}^1 \frac{z'(\frac{r_0 |\sin \varphi_0|}{u})}{\sqrt{1 + r'(z(\frac{r_0 |\sin \varphi_0|}{u}))^2}} \frac{r''(z(\frac{r_0 |\sin \varphi_0|}{u}))}{r'(z(\frac{r_0 |\sin \varphi_0|}{u}))^2} \frac{1}{u \sqrt{1 - u^2}} du. \end{aligned} \quad (13)$$

⁵Because $r' < 0$, we obtain an extra minus sign when moving r' into the square-root.

For convex obstacles, i.e., with $z' < 0$ and $r'' > 0$, the two terms in this expression have opposite signs. The first term < -2 , whereas the second varies between 0 (as $\varphi_0 \rightarrow \pm\pi/2$) and potentially ∞ (as $\varphi \rightarrow 0$). Therefore we cannot expect that $\kappa(\varphi_0)$ is bounded away from $[-2, 0]$ as required in [5] to obtain uniform hyperbolicity.

3.3 Torricelli's trumpets

To simplify formulas in these subsections, we write φ again for φ_0 . Assume that the horn is the surface of revolution of the curve $r(z) = z^{-\beta}$, with $r'(z) = -\beta z^{-(1+\beta)}$, $r''(z) = \beta(1+\beta)z^{-(2+\beta)}$ and $z(r) = r^{-1/\beta}$. Inserting the equations for $r(z)$ into (10) gives $r'(\frac{r_0|\sin\varphi|}{u}) = \beta^{-2}z(\frac{r_0|\sin\varphi|}{u})^{2(1+\beta)} = \beta^{-2}z(\frac{u}{r_0|\sin\varphi|})^{2(1+\beta)/\beta}$ and

$$t_{\max} = \underbrace{|\sin\varphi|^{-\frac{1}{\beta}} \beta^{-1} r_0^{-\frac{1}{\beta}} \int_{|\sin\varphi|}^1 \frac{1}{u^2} \cdot \sqrt{\frac{\beta^2 (r_0 |\sin\varphi|)^{\frac{2(1+\beta)}{\beta}} + u^{\frac{2(1+\beta)}{\beta}}}{1-u^2}}}_{I(\varphi)} du.$$

The integral $I(\varphi)$ tends to a positive constant $I_0 = \beta^{-1} r_0^{-\frac{1}{\beta}} \int_0^{\frac{\pi}{2}} (\sin\alpha)^{\frac{\beta-1}{\beta}} d\alpha$ as $\varphi \rightarrow 0$, so the leading asymptotics of t_{\max} is $|\sin\varphi|^{-1/\beta} I_0$. This gives tails on the height function over base $M_j := -\partial H_j \times [-\frac{\pi}{2}, \frac{\pi}{2}]$,

$$\mu((\theta, \varphi) \in M_j : 2t_{\max} > t) = 2\pi \mu(|\sin\varphi| < (\frac{t}{2r_0 I(\varphi)})^{-\beta}) \sim 4\pi (\frac{t}{2r_0 I_0})^{-\beta}.$$

Applying the same formulas to (11), we get

$$\Delta\theta(\varphi) = \frac{2 \operatorname{sgn}(\varphi)}{(\sin\varphi)^{\frac{1+\beta}{\beta}}} \underbrace{\frac{1}{\beta r_0^{\frac{1+\beta}{\beta}}} \int_{|\sin\varphi|}^1 \sqrt{\frac{\beta^2 (r_0 |\sin\varphi|)^{\frac{2(1+\beta)}{\beta}} + u^{\frac{2(1+\beta)}{\beta}}}{1-u^2}}}_{J(\varphi)} du,$$

and $J(\varphi) \rightarrow \beta^{-1} r_0^{-\frac{1+\beta}{\beta}} \int_0^{\frac{\pi}{2}} (\sin\alpha)^{\frac{1+\beta}{\beta}} d\alpha$ as $\varphi \rightarrow 0$.

Therefore the base map $R : M \rightarrow M$ for base $M_j := \partial H_j \times [-\frac{\pi}{2}, \frac{\pi}{2}]$ becomes

$$R : (\theta, \varphi) \mapsto (\theta + 2 \operatorname{sgn}(\varphi) |\sin\varphi|^{-\frac{1+\beta}{\beta}} J(\varphi), -\varphi).$$

Since $J(\varphi) \rightarrow 0$ as $\varphi \rightarrow \pm\frac{\pi}{2}$ we get $F(\theta, \alpha) \rightarrow (\theta, -\alpha)$ as $\alpha \rightarrow \pm\frac{\pi}{2}$.

Inserting the above into (13), we find

$$\begin{aligned} \kappa(\varphi) &= -2 \operatorname{sgn}(\varphi) \sqrt{1 + \beta^2 r_0^{-2(1+\beta)/\beta}} + \frac{2(1+\beta)}{\beta^2} \frac{r_0^{-(1+\beta)/\beta}}{|\sin\varphi|^{(1+\beta)/\beta} |\tan\varphi|} \times \\ &\quad \int_{|\sin\varphi|}^1 \frac{1}{\sqrt{u^{(1+\beta)/\beta} + \beta^2 (r_0 |\sin\varphi|)^{(1+\beta)/\beta}}} \frac{u^{(1+\frac{1}{\beta})(1+\frac{1}{2\beta})}}{\sqrt{1-u^2}} du. \end{aligned}$$

As φ increases from 0 to $\pi/2$, $\kappa(\varphi)$ decreases from ∞ to $-2\sqrt{1 + \beta^2 r_0^{-2(1+\beta)/\beta}}$, so it smooth with a finite limit as $\varphi \rightarrow \pm\frac{\pi}{2}$, giving the Hölderiness of $\Delta\theta$ away from $\varphi = 0$. However, $\kappa([-\frac{\pi}{2}, \frac{\pi}{2}]) \supset [-2, 0]$ so that hyperbolicity is compromised.

The leading term of $\kappa(\varphi)$, however, is $C\varphi^{-\frac{1+2\beta}{\beta}}$ for some $C > 0$, so, since κ is a smooth function of φ for $\varphi \neq 0$, the leading term of $\kappa'(\varphi)$ in absolute value is

$$\frac{1+2\beta}{\beta}C\varphi^{-\frac{1+3\beta}{\beta}} \leq C\varphi^{-3\frac{1+2\beta}{\beta}} = O(|2+\kappa(\varphi)|) \quad \text{as } \varphi \rightarrow 0,$$

whenever $\beta > -2/3$. Hence, for every $\beta > 0$, item 5. in Section 2.1 holds. By the same token, recalling that $\omega(\varphi) = \frac{2+\kappa(\varphi)}{\cos \varphi}$,

$$\omega'(\varphi) := \frac{\kappa'(\varphi) + (2+\kappa(\varphi))\tan \varphi}{\cos \varphi} \quad \text{is bounded away from 0,}$$

for φ close to 0. Therefore $\omega(\varphi)$ is monotone in one-sided neighborhoods of $\{\varphi = 0\}$, and item 6. in Section 2.1 holds.

3.4 The pseudo-sphere

To treat the pseudo-sphere (which is the surface of revolution of the tractrix), we insert the tractrix into (10): $z(r) = \int_r^1 \frac{\sqrt{1-s^2}}{s} ds$, with $z'(r) = -\frac{\sqrt{1-r^2}}{r}$. Therefore $r'(z) = -\frac{r}{\sqrt{1-r^2}}$. Hilbert's Theorem, see [16] or e.g. [21, Section 11.1], says that the pseudo-sphere is the largest surface of constant curvature $\kappa_G = -1$ that can be embedded in \mathbb{R}^3 .

Inserting these formulas into (10) gives

$$\begin{aligned} t_{\max} &= r_0 |\sin \varphi| \int_{|\sin \varphi|}^1 \frac{1}{\sqrt{1-u^2}} \sqrt{1 + \left(\frac{-r_0 |\sin \varphi|}{u} \right)^2}^{-2} du \\ &= \int_{|\sin \varphi|}^1 \frac{1}{u} \sqrt{\frac{1}{1-u^2}} du = \int_{|\varphi|}^{\frac{\pi}{2}} \frac{1}{|\sin \alpha|} d\alpha \quad (u = \sin \alpha) \\ &= \int_0^{\cos \varphi} \frac{dv}{1-v^2} = \frac{1}{2} \int_0^{\cos \varphi} \frac{1}{1-v} + \frac{1}{1+v} dv \quad (v = \cos \alpha) \\ &= \log \sqrt{\frac{1+\cos \varphi}{1-\cos \varphi}} = \log \left| \frac{1+\cos \varphi}{\sin \varphi} \right|. \end{aligned}$$

Alternatively, see also [21, Example 9.3.3], in the hyperbolic half-plane \mathbb{H} , we can obtain a modular surface by taking the quotient under a Kleinian group $\langle M_t, M_i \rangle$ for the translation $M_t : z \mapsto z + 2\pi$ and involution $M_i : z \mapsto (2\pi)^2/z$. The region $S = [0, 2\pi] + [1, \infty)i$ is then comparable to the pseudo-sphere with boundary $\partial H = [0, 1\pi] \times \{i\}$. A geodesic Γ starting at ∂H making an angle φ with the vertical meridian is then an circular arc of radius $R = 1/\sin \varphi$, connecting $a := (1 - \cos \varphi)R \pmod{2\pi} + iR \sin \varphi = (1 - \cos \varphi)R \pmod{2\pi} + i$ to $b := (1 + \cos \varphi)R \pmod{2\pi} + iR \sin \varphi = (1 + \cos \varphi)R \pmod{2\pi} + i$, see Figure 6. This is part of the semi-circle connection 0 to $2R$, and the the maximal point of this geodesic is $c := (1 + i)R$. To compute the length of this geodesic, we transform it to a vertical arc in \mathbb{H} using the isometry (Möbius transformation)

$$f(z) = \frac{-z}{z - 2R}, \quad \text{so that } f(0) = 0, f(c) = 1 \text{ and } f(2R) = \infty.$$

Then $f(a) = \frac{\sin \varphi}{1 + \cos \varphi} i$ and $f(b) = \frac{\sin \varphi}{1 - \cos \varphi} i$. Therefore the hyperbolic length of Γ is

$$\ell(\Gamma) = \int_{f(a)}^{f(b)} \frac{1}{y} dy = \log \frac{f(b)}{f(a)} = \log \frac{1 + \cos \varphi}{1 - \cos \varphi} = 2 \log \left| \frac{1 + \cos \varphi}{\sin \varphi} \right|.$$

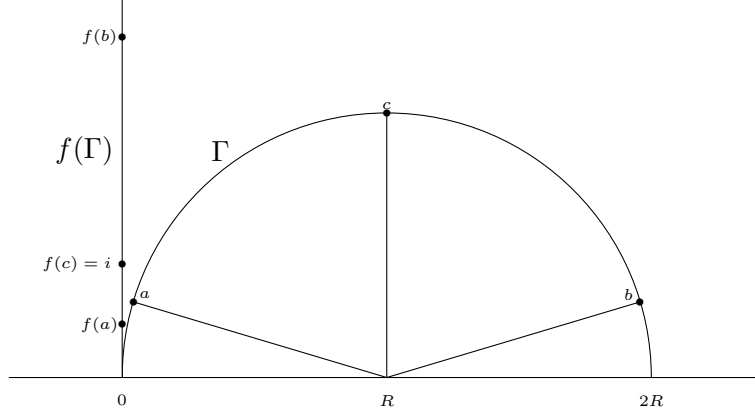


Figure 6: The geodesic Γ and $f(\Gamma)$ in the hyperbolic half-plane \mathbb{H} .

As the unit mass particle goes through this curve at unit speed (in hyperbolic metric), the time it takes to go from a to b is $2t_{\max} = 2 \log \frac{1+\cos \varphi}{\sin \varphi}$.

This gives tails on the height function over base M_j :

$$\mu((\theta, \varphi) \in M_j : 2t_{\max} > t) = 2\pi \mu \left(\left| \frac{\sin \varphi}{1 + \cos \varphi} \right| < e^{-t/2} \right) \sim 8\pi e^{-t/2}.$$

The corresponding reflection map $R : M_j \rightarrow M_j$ is given by

$$R : (\theta, \varphi) \mapsto \left(\theta + \frac{2 \cos \varphi}{\sin \varphi}, -\varphi \right).$$

Again, $R(\theta, \varphi) \rightarrow (\theta, -\varphi)$ as $\varphi \rightarrow \pm \frac{\pi}{2}$. In this case $\Delta\theta = \frac{2 \cos \varphi}{\sin \varphi}$. Hence $\kappa(\varphi) = -2 \sin^{-2} \varphi$ and $\omega(\varphi) = \frac{2-2 \sin^{-2} \varphi}{\cos \varphi}$ are easily seen to satisfy the conditions in Section 2.1, even $\kappa(\varphi) \leq -2$ so it has only one point in common with $[-2, 0]$. Hence, the use of scatterers to regain hyperbolicity of wavefronts remains necessary, but since $\kappa(\varphi) = -2$ only at grazing collisions, it may suffice to stipulate that not more than two grazing collisions can occur directly after one-another, and then there is no need for scatterers.

3.5 The sphere

Assuming again that $r_0 = 1$, the radius of the stunted sphere H centered at the origin containing the circle $\{r = r_0 = 1, z = z_0\}$ as boundary is $R = r_0 \sqrt{1 + r_0'^2}$ and $z_0 = -r_0 r_0'$. This gives a parametrization $r(z) = \sqrt{R^2 - z^2}$, so $r'(z) = \frac{-z}{\sqrt{R^2 - z^2}}$, and $z(r) = \sqrt{R^2 - r^2}$. Inserting this in (10) we obtain

$$\begin{aligned} t_{\max} &= r_0 |\sin \varphi| \int_{|\sin \varphi|}^1 \frac{1}{u} \frac{1}{\sqrt{1-u^2}} \frac{1}{\sqrt{u^2 - r_0^2 R^{-2} \sin^2 \varphi}} du \\ &= r_0 |\sin \varphi| \int_{|\varphi|}^{\frac{\pi}{2}} \frac{1}{\sin \alpha} \frac{1}{\sqrt{\sin^2 \alpha - r_0 R^{-2} \sin^2 \varphi}} d\alpha. \end{aligned}$$

By inserting this curve in (11) gives us the change in θ :

$$\begin{aligned}\Delta\theta(\varphi) &= 2\operatorname{sgn}(\varphi) \int_{|\sin\varphi|}^1 \frac{1}{\sqrt{1-u^2}} \frac{u}{\sqrt{u^2 - r_0^2 R^{-2} \sin^2\varphi}} du \\ &= 2\operatorname{sgn}(\varphi) \int_{|\varphi|}^{\frac{\pi}{2}} \frac{\sin\alpha}{\sqrt{\sin^2\alpha - r_0^2 R^{-2} \sin^2\varphi}} d\alpha,\end{aligned}$$

with corresponding reflection map. Since $\Delta\theta$ is bounded, creating countably many homogeneity regions near $\{\varphi = 0\}$ as in Section 2.3 is not possible, but it is not necessary either, because $R : \varphi \mapsto \Delta\theta(\varphi)$ is a smooth function, with bounded distortion. As $\varphi \rightarrow 0$, $\Delta\theta(\varphi) \rightarrow \pi$ (the geodesic goes over the ‘‘North’’ pole), and as $\varphi \rightarrow \pm\frac{\pi}{2}$, $\Delta\theta(\varphi) \rightarrow 0$ (the geodesic is tangent to ∂H). Since $0 \leq \sin^2\varphi \leq \sin^2\alpha$ in this integrand, we get

$$\frac{\pi - 2|\varphi|}{\sqrt{1 - r_0^2/R^2}} \geq |\Delta\theta| \geq \pi - 2|\varphi| \quad \text{and} \quad \lim_{\varphi \rightarrow \pm 0} \Delta\theta(\varphi) = \pm\pi.$$

The derivative is

$$\kappa(\varphi) = -2\operatorname{sgn}(\varphi)R \cos\varphi \left(\frac{1}{z_0} + r_0^2 \sin\varphi \int_{|\varphi|}^{\frac{\pi}{2}} \frac{\sin\alpha}{(R^2 \sin^2\alpha - r_0^2 \sin\varphi)^{3/2}} d\alpha \right)$$

and this is bounded on $[-\frac{\pi}{2}, \frac{\pi}{2}]$. It tends to $\mp 2\left(\frac{R}{z_0} - \frac{r_0^2}{R^2}\right)$ as $\varphi \rightarrow \pm 0$ (note that $2\left(\frac{R}{z_0} - \frac{r_0^2}{R^2}\right)$ takes its smallest value $2^{4/3} - 2^{1/3} \approx 1.26$ at $z_0 = R/2^{1/3}$), and to ∓ 0 as $\varphi \rightarrow \pm\frac{\pi}{2}$. Hence $\kappa([-\frac{\pi}{2}, \frac{\pi}{2}]) \cap [-2, 0] \neq \emptyset$, so scatterers are required to regain hyperbolicity of wavefronts, but $\kappa(\varphi)$ and

$$\omega(\varphi) = \frac{2 + \kappa(\varphi)}{\cos\varphi} = \frac{2}{\cos\varphi} - 2R \operatorname{sgn}(\varphi) \left(\frac{1}{z_0} + r_0^2 \sin\varphi \int_{|\varphi|}^{\frac{\pi}{2}} \frac{\sin\alpha}{(R^2 \sin^2\alpha - r_0^2 \sin\varphi)^{3/2}} d\alpha \right)$$

satisfy the conditions of Section 2.4.

References

- [1] V. Araújo, I. Melbourne, *Exponential decay of correlations for non-uniformly hyperbolic flows with a $C^{1+\alpha}$ stable foliation*, Ann. Henri Poincaré **17** (2016), 2975–3004.
- [2] A. Avila, S. Gouëzel, J.-C. Yoccoz, *Exponential mixing for the Teichmüller flow*, Publ. Math. Inst. Hautes Etudes Sci. **104** (2006), 143–211.
- [3] V. I. Arnol’d, *Mathematical methods of celestial mechanics*, Springer Verlag, New York Heidelberg Berlin 4th ed. (1984).
- [4] P. Bálint, P. I. Tóth, *Correlation decay in certain soft billiards*, Commun. Math. Phys., **243** (2003) 55-91.
- [5] P. Bálint, P. I. Tóth, *Mixing and its rate in soft and hard billiards motivated by the Lorentz process*, Physica D, **187** (2004) 128-135.
- [6] H. Bruin, D. Terhesiu, *Regular variation and rates of mixing for infinite measure preserving almost Anosov diffeomorphisms*, Ergod. Th. & Dyn. Sys. **40** (2020), 663–698.

- [7] H. Bruin, D. Terhesiu, M. Todd, *Pressure function and limit theorems for almost Anosov flows*, Preprint 2018, arXiv:1811.08293, to appear in Commun. Math. Phys.
- [8] L. Bunimovič, Y. Sinaï, *The fundamental theorem of the theory of scattering billiards*, Mat. Sb. (N.S.) **90** (1973), 415–431, 479.
- [9] N. Chernov, *Decay of correlations and dispersive billiards*, J. Statist. Phys. **94** (1999) 513–556.
- [10] N. Chernov, R. Markarian, *Chaotic billiards*, Mathematical Surveys and Monographs, **127**, Amer. Math. Soc., Providence, RI, 2006.
- [11] Y. Coudène, *Sur le mélange du flot géodésique*, Monogr. Enseign. Math., **43**, Enseignement Math., Geneva, (2013) 13–24.
- [12] Y. Coudène, B. Schapira, *Generic measures for geodesic flows on nonpositively curved manifolds*, J. Ec. Polytech. Math. **1** (2014), 387–408.
- [13] D. Dolgopyat, *On the decay of correlations in Anosov flows*, Ann. of Math. **147** (1998), 357–390.
- [14] V. Donnay, C. Pugh, *Anosov geodesic flows for embedded surfaces*, Geometric methods in dynamics. II. Astérisque **287** (2003), 61–69.
- [15] G. Gallavotti, D. Ornstein, *Billiards and Bernoulli schemes*, Commun. Math. Phys. **38**(1974), 83–101.
- [16] D. Hilbert, *Über Flächen von konstanter Krümmung*, Trans. Amer. Math. Soc. **2** (1901), 87–99.
- [17] H. Hu, *Conditions for the existence of SBR measures of “almost Anosov” diffeomorphisms*, Trans. Amer. Math. Soc. **352** (2000) 2331–2367.
- [18] H. Hu, X. Zhang, *Polynomial decay of correlations for almost Anosov diffeomorphisms*, Ergod. Th. & Dyn. Sys. **39** (2019), 832–864.
- [19] I. Melbourne, P. Varandas, *Convergence to a Levy process in the Skorohod \mathcal{M}_1 and \mathcal{M}_2 topologies for nonuniformly hyperbolic systems, including billiards with cusps*, Commun. Math. Phys. **375** (2020) 653–678.
- [20] M. Pollicott, H. Weiss, *Ergodicity of the geodesic flow on non-complete negatively curved surfaces*, Asian J. Math. **13** (2009), 405–419.
- [21] A. Pressley, *Elementary differential geometry*, 2nd ed. Springer-Verlag, London (2010).
- [22] Y. Sinaï, *Dynamical systems with elastic reflections: Ergodic properties of dispersing billiards*, Russ. Math. Surv. **25** (1970), 137–189.
- [23] L.-S. Young, *Statistical properties of dynamical systems with some hyperbolicity*, Ann. of Math. **147** (1998) 585–650.
- [24] L.-S. Young, *Recurrence times and rates of mixing*, Israel J. Math. **110** (1999) 153–188.